

# Attenuated Human Bone Morphogenetic Protein-2–Mediated Bone Regeneration in a Rat Model of Composite Bone and Muscle Injury

Nick J. Willett, PhD,<sup>1</sup> Mon-Tzu A. Li, BS,<sup>1</sup> Brent A. Uhrig, BS,<sup>1</sup> Joel David Boerckel, PhD,<sup>1</sup>  
Nathaniel Huebsch, PhD,<sup>2,3</sup> Taran S. Lundgren, BA,<sup>1</sup> Gordon L. Warren, PhD,<sup>4,5</sup>  
and Robert E. Guldberg, PhD<sup>1</sup>

Extremity injuries involving large bone defects with concomitant severe muscle damage are a significant clinical challenge often requiring multiple treatment procedures and possible amputation. Even if limb salvage is achieved, patients are typically left with severe short- and long-term disabilities. Current preclinical animal models do not adequately mimic the severity, complexity, and loss of limb function characteristic of these composite injuries. The objectives of this study were to establish a composite injury model that combines a critically sized segmental bone defect with an adjacent volumetric muscle loss injury, and then use this model to quantitatively assess human bone morphogenetic protein-2 (rhBMP-2)–mediated tissue regeneration and restoration of limb function. Surgeries were performed on rats in three experimental groups: muscle injury (8-mm-diameter full-thickness defect in the quadriceps), bone injury (8-mm nonhealing defect in the femur), or composite injury combining the bone and muscle defects. Bone defects were treated with 2  $\mu$ g of rhBMP-2 delivered in the pregelled alginate injected into a cylindrical perforated nanofiber mesh. Bone regeneration was quantitatively assessed using microcomputed tomography, and limb function was assessed using gait analysis and muscle strength measurements. At 12 weeks postsurgery, treated bone defects without volumetric muscle loss were consistently bridged. In contrast, the volume and mechanical strength of regenerated bone were attenuated by 45% and 58%, respectively, in the identically treated composite injury group. At the same time point, normalized muscle strength was reduced by 51% in the composite injury group compared to either single injury group. At 2 weeks, the gait function was impaired in all injury groups compared to baseline with the composite injury group displaying the greatest functional deficit. We conclude that sustained delivery of rhBMP-2 at a dose sufficient to induce bridging of large segmental bone defects failed to promote regeneration when challenged with concomitant muscle injury. This model provides a platform with which to assess bone and muscle interactions during repair and to rigorously test the efficacy of tissue engineering approaches to promote healing in multiple tissues. Such interventions may minimize complications and the number of surgical procedures in limb salvage operations, ultimately improving the clinical outcome.

---

Portions of this article were presented at the following conferences:

Willett NJ, Li MA, Uhrig BA, Warren GL, Guldberg RE. "BMP-2 Mediated Tissue Regeneration in a Composite Rat Injury Model." Tissue Engineering and Regenerative Medicine International Society-NA Meeting, Houston, TX, December, 2011.

Willett NJ, Li MA, Uhrig BA, Warren GL, Guldberg RE. "Muscle Injury Attenuates BMP-2 Mediated Tissue Regeneration in a Novel Rat Model of Composite Bone and Muscle." American Society For Mechanical Engineering Summer Bioengineering Conference, Farmington, PA, June 2011.

Willett NJ, Li MA, Uhrig BA, Warren GL, Guldberg RE. "Functional and Structural Analysis of Limb Restoration Using a Novel Rat Model of Composite Bone and Muscle Injury." Orthopedic Research Society Conference, Long Beach, CA, January 2011.

<sup>1</sup>George W. Woodruff School of Mechanical Engineering, Petit Institute for Bioengineering and Bioscience, Georgia Institute of Technology, Atlanta, Georgia.

<sup>2</sup>School of Engineering and Applied Sciences, Harvard University, Cambridge, Massachusetts.

<sup>3</sup>Wyss Institute for Biologically Inspired Engineering, Cambridge, Massachusetts.

<sup>4</sup>Division of Physical Therapy, Georgia State University, Atlanta, Georgia.

<sup>5</sup>School of Applied Physiology, Georgia Institute of Technology, Atlanta, Georgia.

## Introduction

THERE IS GROWING appreciation of the profound interactions between the skeletal muscle and bone during development, daily function, and healing subsequent to traumatic injury. Clinical studies have reported that composite injuries consisting of both bone fracture and muscle injury significantly complicate fracture healing, often resulting in delayed healing, nonunion, infection, re-hospitalization, and additional surgeries.<sup>1–5</sup> Coverage of an open fracture with a muscle flap is the clinical gold standard for intervention and has been shown to improve fracture healing, suggesting that muscle somehow contributes to the bone repair process.<sup>6–8</sup> Medical advances have made limb salvage common after these severe injuries; however, patients are often left with substantial short-term and long-term disabilities.<sup>5,9</sup> Although long-term function at 2 and 7 years postinjury is approximately equivalent in amputation and limb salvage patients (based on the sickness impact profile scoring system), amputees are at a lower risk for further complications or additional surgeries.<sup>5,9</sup> Additionally, functional disabilities, pain, neurologic dysfunction, and infection can result in delayed amputations at reported rates of 4%–15% in limb salvage cases involving severe bone (grade III) and soft tissue injury (crush or volumetric muscle loss).<sup>10–12</sup> Although limb salvage techniques have improved, there are substantial advancements still to be made in limb reconstruction and rehabilitation leading to the restoration of normal function. Highlighting this need, composite extremity injuries are the leading battlefield injuries faced by returning servicemen.<sup>10,13,14</sup> To date, clinical composite injury studies have been mainly observational in nature without offering clear insight into the mechanisms involved.

Potential roles for muscle in bone healing include acting as a source for vascularization, progenitor cells, osteogenic myokines, and also biomechanical stimuli.<sup>15,16</sup> Studies have shown that muscle surrounding a bone defect contributes to re-establishing the blood supply, a step that is critical to ensure successful bone healing.<sup>17–19</sup> Additionally, muscle cells secrete numerous osteogenic factors (including insulin-like growth factor [IGF]-1, fibroblast growth factor [FGF]-2, and transforming growth factor [TGF]- $\beta$ ) under basal conditions, with increased secretion in regenerating muscle.<sup>16,20,21</sup> The periosteum, a cellular membrane that separates bone and muscle tissues, expresses receptors for these growth factors suggesting a mechanism of tissue cross talk.<sup>16</sup> These growth factors have also been implicated in the recruitment and differentiation of osteogenic progenitor cells. Muscle progenitor cells have also demonstrated a capability to differentiate into osteogenic cell lineages.<sup>22,23</sup> A recent study tracked these muscle progenitor cells after an open bone fracture and showed incorporation of these cells in regenerated bone.<sup>24</sup> These studies have demonstrated potential mechanisms of interaction between bone and muscle during regeneration.

There are currently few models of composite bone–muscle injury in the literature and no models that can be used to assess multi-tissue engineering strategies. The few models in the literature have all been performed in the lower limb and combine a naturally healing fracture or osteotomy with varying degrees of muscle injury (laceration, crush, or resection).<sup>7,25–27</sup> Models with a severe muscle injury (resection)

typically displayed delayed bone healing, while models with less severe muscle injuries commonly displayed no effect on bone healing. A recent consensus recommendation published by experts in the fracture field pointed to the thin soft tissue coverage of the tibia as a reason that it may not be an ideal location to investigate the relation of soft tissue to bone repair.<sup>28</sup> Instead, the femur was recommended due to thick muscle coverage. In addition, a fracture model has limited utility for the investigation of tissue-engineered bone constructs, which are typically assessed in critically sized, nonhealing defects. To effectively develop and evaluate tissue-engineered constructs for multi-tissue limb reconstruction, a more challenging preclinical model of traumatic injury is needed as are quantitative functional outcome measures.

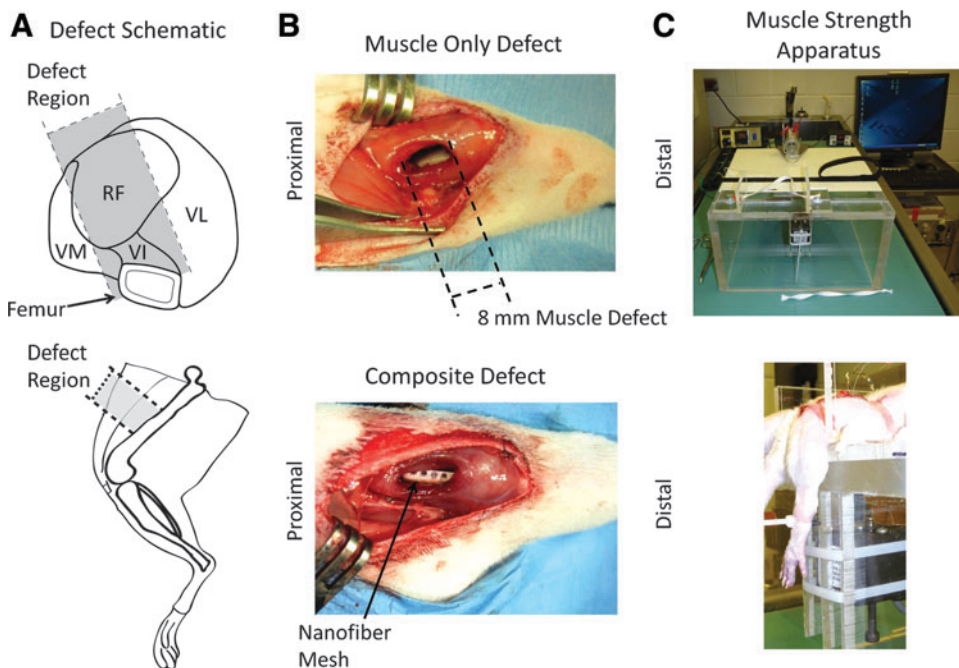
In this study, we developed a composite injury model consisting of a critically sized segmental bone defect in the femur and an adjacent volumetric muscle injury in the quadriceps. An established tissue-engineered recombinant human bone morphogenetic protein-2 (rhBMP-2) delivery system was tested for the treatment of the bone defect.<sup>29–31</sup> This system had previously been shown to provide sustained delivery of rhBMP-2 at a dose sufficient to induce bridging of a bone defect in a single tissue injury model.<sup>29–31</sup> It was hypothesized that animals with a composite injury would have attenuated tissue regeneration and impaired limb function despite rhBMP-2 treatment. This model can be used to test the efficacy of novel treatments for composite injuries and will also provide insight into the mechanisms by which muscle and bone interact during regeneration.

## Materials and Methods

### *Surgical procedure*

Thirteen-week-old-female Sprague-Dawley rats (Charles River Labs) were used for this study. Animals were placed in one of the three injury groups: bone defect only ( $n=5$ ), muscle defect only ( $n=8$ ), or composite bone and muscle defect ( $n=5$ ). Unilateral bone defects were surgically created in the femora of rats, as previously described.<sup>30–32</sup> Briefly, an anterior incision was made along the length of the femur and the muscle was then separated using blunt dissection. A modular fixation plate was affixed to the femur using miniature screws (JI Morris Co., Part No. P0090CE250). A full-thickness segmental defect, 8 mm in length, was created in the diaphysis using a miniature oscillating saw. A perforated nanofiber mesh tube was then placed over the native bone ends surrounding the defect, and 150  $\mu$ L alginate hydrogel containing 2.0  $\mu$ g rhBMP-2 was then injected into the defect space.<sup>31</sup> This dose had previously been shown to consistently induce bridging of the bone defect.<sup>29,32</sup> Nontreated controls were not used in this study as previous studies have demonstrated that in the absence of rhBMP-2, the defect contains very little bone formation.<sup>29,32</sup> Muscle defects were created through the full thickness of the quadriceps down to the femur using an 8-mm-diameter biopsy punch (Fig. 1A). The defect encompassed regions of the rectus femoris, vastus lateralis, vastus medialis, and vastus intermedius. The muscle defect was untreated in this study and left empty. In composite injury animals, the bone defect was made first, then, once the incised muscles had been closed with 4-0 suture, the muscle defect was created. Animals were given buprenorphine postsurgery to manage pain (0.03 mg/kg 3  $\times$

**FIG. 1.** Representative Methods Images—(A) shows schematic illustrations of the anatomical injury location, including a cross section through the quadriceps (top) and a side view of the hindlimb (bottom). (B) shows images from the muscle defect only surgery (top) and the composite bone and muscle defect surgery (bottom). (C) shows representative images of the muscle strength-measuring apparatus (top) and positioning of a rat limb in the apparatus (bottom). The animal was secured at the hips and the knee by a strap, and then the ankle was fastened to a force transducer. VM, Vastus Medialis; RF, Rectus Femoris; VI, Vastus Intermedius; VL, Vastus Lateralis. Color images available online at [www.liebertpub.com/tec](http://www.liebertpub.com/tec)



daily for the first 48 h, then 0.01 mg/kg  $3\times$  for the next 24 h). All procedures were approved by the Georgia Institute of Technology Institutional Animal Care and Use Committee (protocol #A09039).

#### Functional gait analysis

Hind limb function was assessed after injury using the CatWalk system (CatWalk 7.1; Noldus Inc.) at baseline (1 week before surgery) and at 2, 4, 8, and 12 weeks postinjury. The system consisted of an illuminated platform, an enclosed walkway, and a digital camera mounted below the platform. The rats were placed at the open end of the track and allowed to ambulate freely to the other end. Illuminated paw prints were recorded and the paw print area and duty cycle were assessed for each group. The paw print area is a static parameter that measures the area of contact that the paw makes with the glass walkway during the stance phase. Duty cycle is a dynamic parameter indicative of limb use during ambulation, and is represented as the ratio of the stance duration to the sum of the stance and swing duration (stride duration).

#### Muscle isometric tetanic torque assessment

Isometric tetanic torque production about the knee by the knee extensor muscles was measured at 12 weeks post-surgery using a custom-built apparatus based on a previous design used for assessment of lower leg muscle function (Fig. 1B).<sup>33</sup> All measurements were made under isoflurane anesthesia during a terminal procedure immediately before euthanasia. A 2-cm-long incision was made through the skin exposing the femoral triangle in the upper thigh. The posterior branch of the femoral nerve was carefully isolated and a nerve cuff was positioned surrounding that branch. The rat

was then carefully secured to the platform of the apparatus. The animal was positioned so that the knee angle was at  $90^\circ$  and the ankle was secured to a force transducer (Isometric Transducer Model No. 60-2996, Harvard Apparatus). The knee extensor muscles were stimulated using a stimulator (GRASS S11 Stimulator, Grass Technologies) and the nerve cuff implanted on the femoral nerve. Stimulator pulse duration, frequency, and train duration were set to 0.5 ms, 175 Hz, and 500 ms, respectively; these settings elicited maximal isometric tetanic torque as determined in a pilot study. Measurements of injured muscles were normalized to the contralateral intact muscle for each animal. A fatigue protocol was run using 60 Hz stimulation for 330 ms every second for 2 min. Fatigue was calculated as the ratio of the force produced at the end of the 2-min protocol compared to the highest force, which typically occurred in the first few seconds of the protocol.

#### Faxitron X-ray analysis

Digital radiographs (Faxitron MX-20 Digital; Faxitron X-ray Corp.) of the defect region in the femur were performed at an exposure time of 15 s and a voltage of 25 kV. Animals received X-ray imaging at 2, 4, 8, and 12 weeks postsurgery. Blinded analysis of bridging rates at 12 weeks was performed by three researchers.

#### Microcomputed tomography analysis

Microcomputed tomography (microCT) scans (Viva-CT 40, Scanco Medical) were performed at  $38.0\text{-}\mu\text{m}$  voxel size at a voltage of 55 kVp and a current of  $109\text{ }\mu\text{A}$ . Scans were taken at 4 and 12 weeks postsurgery. Bone tissue was segmented by application of a global threshold corresponding to  $386\text{ mg hydroxyapatite}/\text{cm}^3$  (roughly 50% of the native

cortical bone density), and a low-pass Gaussian filter ( $\sigma=1.2$ ,  $\text{support}=1$ ) was used to suppress noise. Samples were contoured and evaluated over 141 slices taken from a central region within the defect to normalize between samples without including cortical bone. *Ex vivo* analysis over the entirety of the defect region was also performed and showed the same differences among the groups as the *in vivo* data at 12 weeks.

### Biomechanical analysis

Animals were euthanized by CO<sub>2</sub> inhalation 12 weeks postsurgery. This time point was chosen based on previous publications demonstrating that bone apposition reaches a plateau by this time.<sup>29</sup> Torsional testing was performed on extracted femurs. The femurs were cleaned of soft tissue and the ends potted in mounting blocks using Wood's metal (Alfa Aesar). After removal of the fixation plate, the specimens were tested (ELF 3200; Bose ElectroForce Systems Group) at a rotational rate of 3° per second. Maximum torque was measured at the failure point from the torque rotation data. Torsional stiffness was calculated by fitting a straight line to the linear portion of the curve before failure.

### Histology

Histological analysis was performed at 12 weeks postsurgery on extracted quadriceps, muscles, or femurs. Samples were perfusion fixed, and then immersion fixed for 48 h at 4°C with 10% neutral-buffered formalin. Following paraffin processing, 5- $\mu\text{m}$ -thick cross-sections were cut and stained with hematoxylin and eosin (H&E), 0.5% Safranin-O (for bone), or Masson's Trichrome (for muscle). Bright-field images were obtained with the Axio Observer Z1 microscope (Carl Zeiss). Images were taken at 4 $\times$  and 10 $\times$  magnification using the AxioVision software (Carl Zeiss).

### Statistical analysis

All data are presented as mean  $\pm$  standard error of the mean (SEM). Differences between multiple groups were assessed by analysis of variance (ANOVA) or for analyses with only two groups, the Student's *t*-test or the Mann-Whitney test were used. A Tukey *post hoc* comparison was performed on the muscle and bone regeneration data, while the gait data was assessed with the Bonferroni *post hoc* test with pairwise comparisons within groups across time points or within time points across groups. A *p*-value less than 0.05 was considered significant. GraphPad Prism 5 (GraphPad Software, Inc.) was used to perform the statistical analysis. One sample was removed from the control bone defect group as an outlier. Bone volume, stiffness, and failure

strength from this sample were over two standard deviations from the mean for the group (and from historical values for over 20 samples).<sup>29</sup>

## Results

### Bone regeneration

Faxitron X-ray radiographs were taken at 2, 4, 8, and 12 weeks postsurgery and illustrated the progression of bone formation in each group (Fig. 2). Blinded analysis of bridging rates showed that the defect was bridged at 12 weeks in all animals with bone-only defects, while only three of six animals in the composite group showed bridging of the defect.

MicroCT quantification of bone formation was performed at 4 and 12 weeks postsurgery (Fig. 3A, B). At week 4, there were no significant differences between the groups though there was a trend for attenuated bone formation in the composite injury group. Animals in both groups had a significant increase in bone formation in the defect region between 4 and 12 weeks. By week 12, the composite injury animals had 45% less bone volume formed in the defect region as compared to animals in the bone injury-only group, a significantly lower value.

The degree of functional restoration in the regenerated bone tissue was measured using torsional testing to failure (Fig. 3C). The composite injury group had a significantly lower failure torque (59% lower) and stiffness (87% lower) as compared to the bone from animals in the bone-only injury group.

Histological assessment of bone quality and composition was performed using H&E and Safranin-O staining (Fig. 4). Bone injury animals showed areas of bone formation and endochondral ossification with larger well-defined pockets of alginate when present. Composite injury animals showed some bone formation, though endochondral ossification was not observed. Alginate was present throughout the bone defect region in smaller pockets integrated within the regenerated bone.

### Muscle regeneration

Muscle regeneration was assessed histologically using H&E and Masson's Trichrome staining. Masson's Trichrome stain from the composite injury group showed fibrosis surrounding individual muscle fibers and fat nodules, indicating poorly regenerated muscle (Fig. 5B). Animals from the muscle injury-only group showed a band of fibrosis through the central region, while fibrosis was not apparent in the bone-only injury group. Animals in all three groups primarily showed peripherally located nuclei in muscle fibers throughout the H&E stained tissue cross sections, indicating that most muscle fibers were mature and not regenerating 12 weeks postinjury (Fig. 5A).

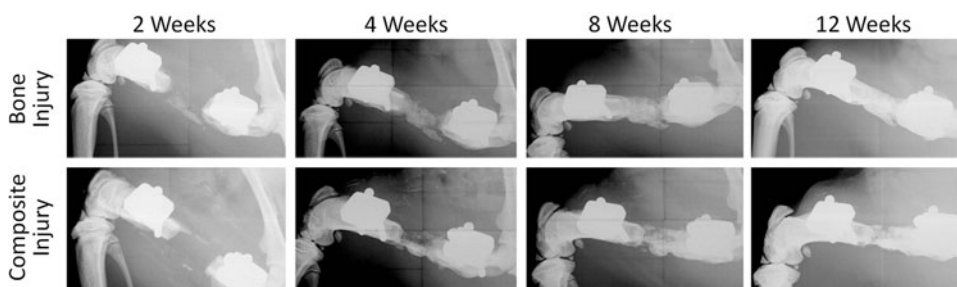
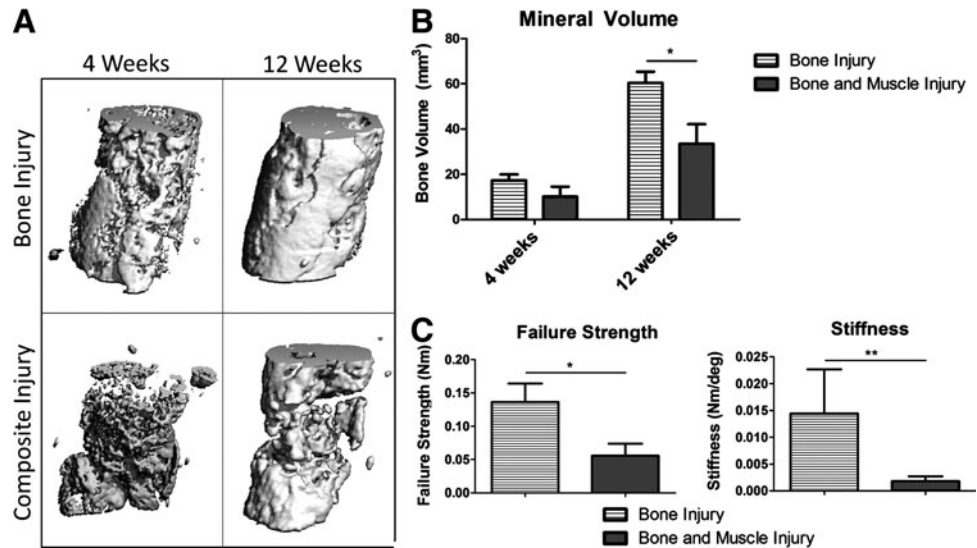


**FIG. 2.** Femur Radiographs—Representative radiographs of the femurs from bone defect and composite defect animals at time points 2, 4, 8, and 12 weeks.

**FIG. 3.** Bone Regeneration (A) shows representative microcomputed tomography reconstructions at 12 weeks from the defect regions of bone defect and composite defect animals. Quantitative measurements of mineral volume in the defect region are presented in (B). Mechanical data showing failure strength and stiffness acquired from torsional testing to failure are presented in (C). \* $p < 0.05$ ; \*\* $p < 0.05$  using a Mann–Whitney test,  $n = 5–8$ .



Muscle regeneration was assessed by measuring isometric torque produced around the knee, which is a direct measure of quadriceps strength (Fig. 6A). Representative force-time tracings during femoral nerve stimulation are presented. All groups showed a significant decrease in muscle strength as compared to the contralateral control limb, 12 weeks post-injury. Strength in the injured limbs was 38% and 18% of the contralateral control in the bone-only defect group, the muscle-only group, and the composite group, respectively. Normalizing the strength of the injured limb by that of the contralateral control limb showed that animals with a composite injury had a significantly greater deficit in muscle strength as compared to animals with a single tissue injury (51% greater deficit). Fatigue waveforms showed normal profiles with a peak in force produced shortly after initial stimulation, and then slowly dropping off (Fig. 6B). Compared to contralateral controls, muscle fatigue was signifi-

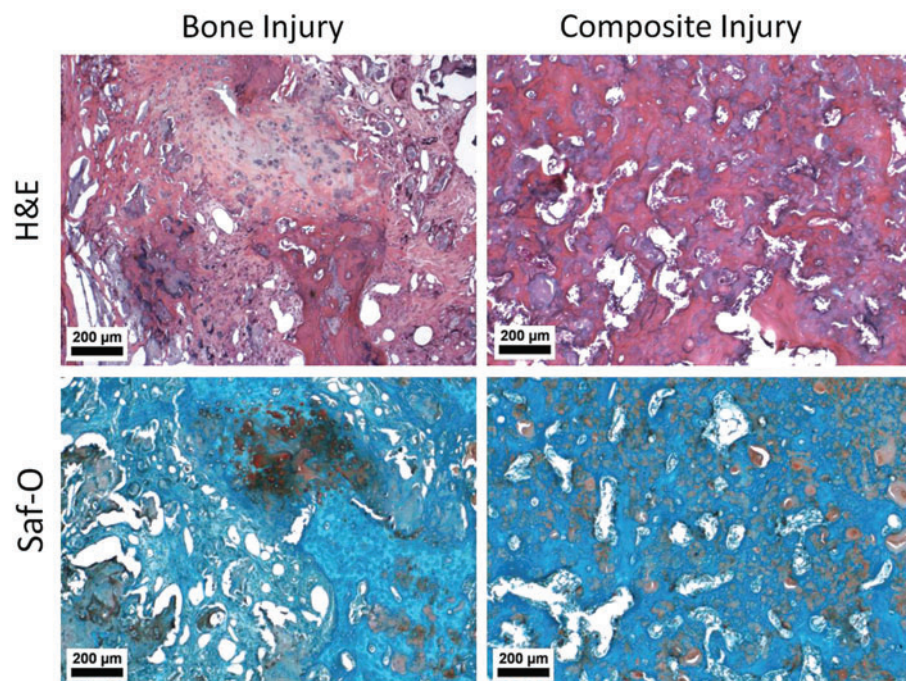
cantly decreased in animals with muscle-only injuries, but not the bone-only or composite injury groups.

Mass of the knee extensor muscle group was measured immediately after euthanizing the animals. All three groups showed a significant reduction in muscle mass in the injured limb as compared to the contralateral control limb (Fig. 6C). Normalized muscle mass (ratio of the mass of the injured limb to that of the contralateral control limb) in the composite injury animals was significantly lower compared to the muscle injury group, but not the bone injury.

*Limb function*

Limb function was quantitatively evaluated by measuring two gait parameters: the paw print area and duty cycle (Fig. 7). All groups, including bone injury, muscle injury, and composite injury, showed a significant deficit in the paw

**FIG. 4.** Bone Histology—Representative hematoxylin and eosin (H&E) and Safranin-O images are presented from within the bone defect region. Bone injury animals showed pockets of hypertrophic chondrocytes indicative of endochondral ossification from Saf-O staining and few larger isolated pockets of alginate. Composite injury animals had smaller pockets of alginate dispersed throughout the defect region as identified in both Saf-O (glossy light pink) and H&E (glossy purple) staining. All images were from 12 weeks postsurgery. Color images available online at [www.liebertpub.com/tc](http://www.liebertpub.com/tc)



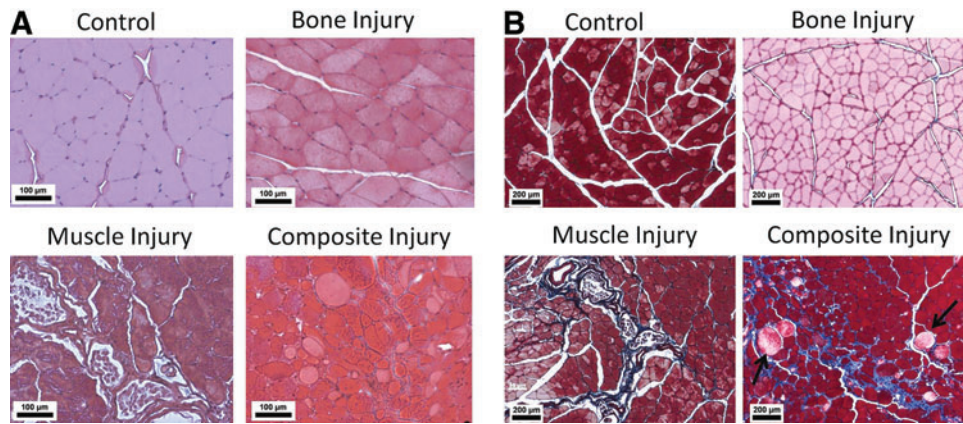


**FIG. 5.** Muscle Histology—(A) shows representative H&E images from quadriceps muscle sections taken from control, bone injury, muscle injury, or composite injury animals. Most muscle fibers showed peripherally located nuclei indicating mature fibers and minimal muscle regeneration at this time point. (B) shows representative Masson's trichrome images from sections adjacent to the images in (A). Blue staining shows fibrosis and the black arrows point to lipid deposits. Both fibrosis and lipid deposits were observed in the composite injury animals indicating poorly regenerated muscle. All images shown were from 12 weeks postsurgery. Color images available online at [www.liebertpub.com/tec](http://www.liebertpub.com/tec)

print area at 2 weeks postsurgery compared to baseline values. The print area deficit observed at 2 weeks was significantly worse in composite injury animals compared to the single tissue injury animals. The composite injury animals showed a steady recovery in the print area between 2 and 12 weeks, reaching a comparable level to the deficit observed in the single tissue injury animals. Similarly, the composite injury animals had a deficit in duty cycle at 2 weeks compared

to baseline values and compared to single tissue injury animals at the same time point. By 4 weeks, duty cycle showed no significant differences among any of the groups.

**Discussion**

Traumatic injuries that create large bone defects often include damage to the surrounding soft tissues. Modern

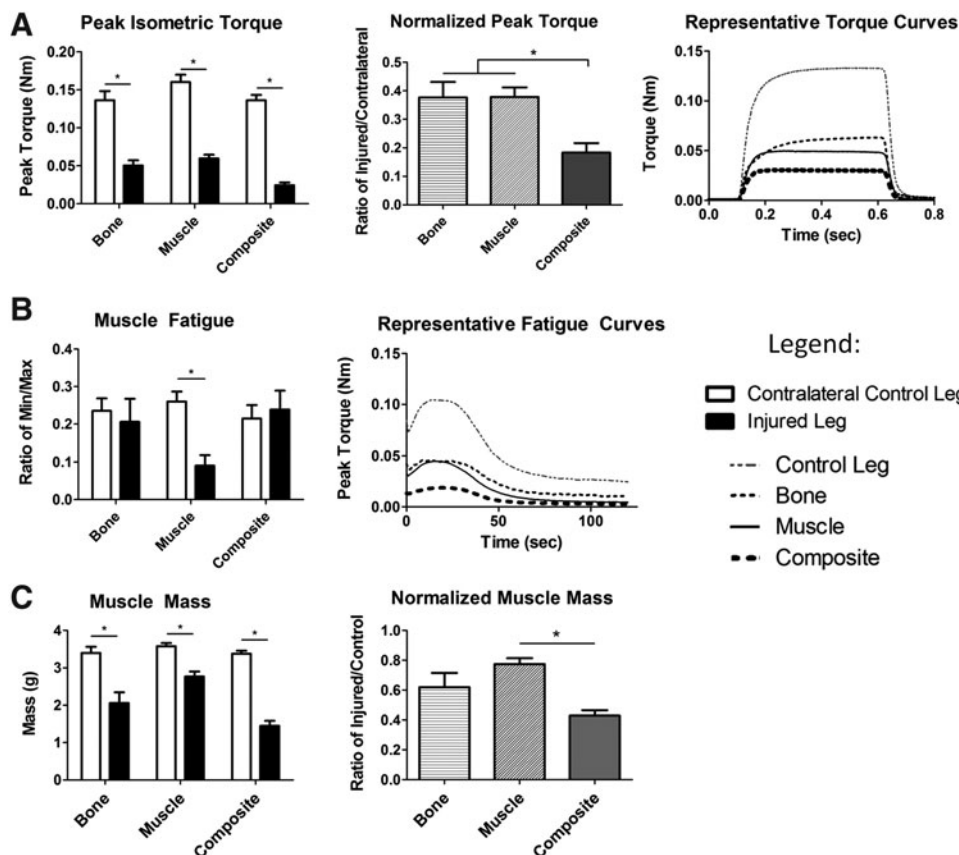
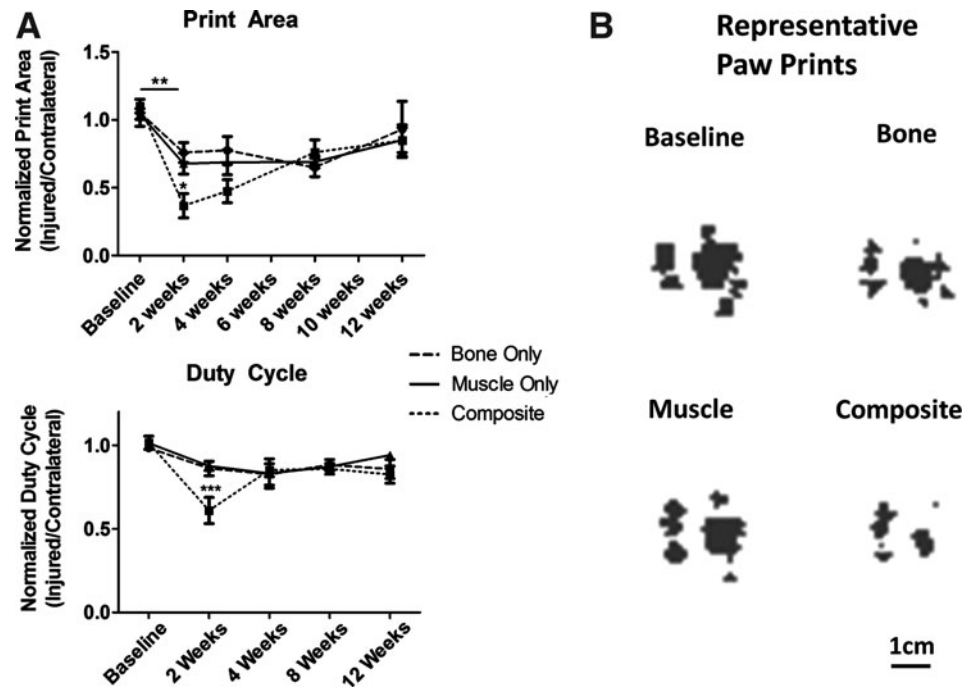


**FIG. 6.** Muscle Functional Capacity— (A) presents peak torque data from animals in all groups at 12 weeks postsurgery including; peak isometric torque (left) in injured and contralateral nonoperated control limb. Normalized torque (center) as the ratio of the peak torque in the injured limb compared to the peak torque in the contralateral nonoperated limb, and representative torque curves (right). (B) shows representative fatigue curves (right) and muscle fatigue data (left) Muscle fatigue was measured for each animal as the ratio of the minimum peak torque compared to the maximum peak torque for each limb. (C) shows the wet muscle mass from the quadriceps immediately after euthanasia. Mass (left) and normalized mass are presented (right). \* $p < 0.05$ ,  $n = 5-8$ .

**FIG. 7.** Limb Function—Measurements of gait were made using the Noldus Catwalk system. Print area and duty cycle (ratio of the stance duration to the sum of the stance and swing duration) at 2-week intervals from animals in all groups are presented in (A). Data is presented as the ratio of the injured limb to the contralateral noninjured control limb. (B) shows representative paw prints, corresponding to the paw print area from the injured limb of animals 2 weeks postsurgery. \* $p < 0.05$  between groups within time point, \*\* $p < 0.05$  between time points within group, \*\*\* $p < 0.05$  compared to baseline within group and within time point between groups,  $n = 5-8$ .



clinical techniques have improved the rates of success in limb salvage; however, patients still requiring repeated hospitalizations for multiple surgeries and complications during the healing process, such as nonunion or infection, are common.<sup>2,3,5</sup> Even when limb salvage is successful, patients are often left with large functional deficits. The complexity, severity, and loss of limb function associated with these injuries are not represented by current preclinical animal models limiting the utility of these models to test the efficacy of tissue-engineered interventions. In this study, we developed a challenging rat model of composite bone and muscle injury by combining a critically sized segmental bone defect model with an adjacent volumetric muscle defect. We then tested the efficacy of a hybrid rhBMP-2 delivery system to regenerate bone and restore limb function.

Preclinical animal models of composite injury have previously been limited to lower limb tibial fractures and, thus, have lacked the capability to assess tissue engineering interventions for multi-tissue limb reconstruction. In this study, we incorporated a well-established, larger than critically sized, segmental bone defect in the femur of a rat. The 8-mm defect used in this model is 60% larger than the necessary critical size, 5 mm, and provides a more challenging regenerative environment; smaller defects could also be combined with an adjacent volumetric muscle injury, and would provide valuable information on the relative importance of defect size (surface area in contact between the bone and muscle) and insight into potential mechanisms of interaction. We have previously demonstrated the efficacy of a sustained release, hybrid rhBMP-2 delivery system, showing consistent bridging of the bone defect with doses of rhBMP-2 as low as 1.0  $\mu\text{g}$ .<sup>29</sup> This system previously outperformed the clinical gold standard for rhBMP-2 delivery, absorbable collagen sponge. Furthermore, the dose used was at the low end of doses commonly reported in similar rat models, which typically range from 2 to 20  $\mu\text{g}$ .<sup>29-32,34-38</sup> Consistent with previously published data, the current study showed that the

hybrid rhBMP-2 delivery system promoted consistent bone bridging in the bone-only injury model.<sup>29</sup> At 12 weeks, animals in the composite injury group had significantly attenuated rhBMP-2-mediated bone regeneration compared to the bone-only injury group, both in terms of mineralized matrix volume and mechanical strength. In this new composite injury model, which utilizes a segmental bone defect, it was demonstrated that a healing dose of rhBMP-2 sufficient to bridge a large bone defect, failed to promote regeneration when challenged with a concomitant volumetric muscle injury.

The surrounding soft tissue may be expected to play a larger role in the healing of a femoral segmental bone defect compared to the previously used tibial fracture. This may simply be due to the relative distance of the defect region to the muscle as opposed to the periosteum. Fractures primarily heal through endochondral bone repair, a process largely directed by the periosteum.<sup>39-42</sup> The contribution of muscle-derived cells to fracture healing was recently demonstrated by tracking muscle-derived cells (MyoD-Cre<sup>+</sup>).<sup>24</sup> After a closed fracture, very few muscle-derived cells were present in the fracture callus, however, after an open fracture with the adjacent periosteum denuded, there was a substantial population of muscle-derived cells in the callus, fracture gap, and pericortical bone.<sup>24</sup> This study speculated that the periosteum is sufficient for fracture healing, and when present, other sources for osteoprogenitor cells are not necessary. In critically sized segmental defects, the periosteum is not sufficient to direct healing and the natural healing progression will instead cap off the cortical bone ends. During rhBMP-2-mediated healing of segmental defects the relative contribution of various cell sources is unknown; however, new models, like the one presented in this study, will provide tools to address these gaps in the current understanding of bone regeneration.

The deleterious effects of concomitant muscle injury on bone regeneration may be attributable to numerous potential

mechanisms, which have not yet been fully elucidated. One potential mechanism may be a diminished blood supply, which has been shown to be a risk factor for successful healing of a bone defect.<sup>43</sup> The large volumetric muscle defect was from a highly vascularized region of tissue. Beyond, simply a loss in normal blood supply, there may be hyperemia through the collateral network immediately following the bone defect injury. This altered blood supply (whether normal or hyperemic) in the muscle defect animals may produce changes in nutrient and waste exchange, inflammation, circulating stem cell recruitment, and ultimately, revascularization of the defect. Another potential mechanism may be that the loss of muscle volume removes a source for resident muscle stem cells and myokines (including IGF-1, FGF-2, or TGF- $\beta$ ) which may contribute locally to bone regeneration. While these factors and cells are key components to muscle regeneration they have also been shown to have osteogenic capabilities.<sup>16,21-23</sup> There is also an increasing body of literature that suggests that muscle may act systemically on other organs, potentially through neural feedback or endocrine type mechanisms.<sup>44,45</sup> Studies on injury, hindlimb unloading, and paralysis implicate both systemic and local roles for muscle in bone homeostasis, though the exact mechanisms are still unclear.<sup>44,46,47</sup> Restoration of a vascular supply, muscle-derived stem cells, or growth factors all may be targets for tissue engineering interventions of composite injuries. An improved understanding of the mechanisms and timing of bone, muscle, and vasculature interactions involved in tissue regeneration will be valuable to inform the development of multi-tissue interventions.

Composite injury animals had impaired muscle regeneration in addition to the impaired bone regeneration. These animals showed decreased muscle mass and impaired muscle function compared to single tissue injury animals. The decrease in mass may be attributable to a loss in volume from the defect as well as potential muscle atrophy. In the bone defect-only animals, there was a significant decrease in muscle mass potentially as a result of decreased limb function or the presence and volume of the fixation plate. The decreased muscle mass may account for some of the decreased function; however, in all three groups, the relative proportion of muscle mass lost was less than the relative decrease in muscle strength. This suggests that there was also a loss of functional capacity that may be due to poor muscle structure. Histology of muscle from the composite injury animals showed poorly regenerated tissue with fibrosis and lipid deposits. The local fibrotic response in the muscle tissue can result in increased local concentrations of fibrotic factors, such as TGF- $\beta$ , tissue inhibitor of matrix metalloproteinase, and chemokine ligand 17.<sup>48,49</sup> These factors may reach the bone defect region and could direct a fibrotic response instead of bone regeneration.<sup>49</sup> Additionally, the impaired muscle function may have an effect on the bone regeneration as muscle atrophy and wasting are both associated with negative changes in bone structure and osteoporosis.<sup>44,50,51</sup> The bone defect itself, however, is largely stress shielded by fixation hardware, precluding a direct mechanical loading effect.

Composite injury animals showed functional gait deficits in injured limbs compared with single tissue injury animals at 2 weeks. By 4 weeks, composite injury animals had deficits that were comparable to single tissue injury deficits. These

functional deficits could have a direct effect on limb usage and, ultimately, tissue regeneration. A limitation of this technique is that these measurements assess functional gait ability (i.e., how well the animal can walk) at a given time, but are not necessarily indicative of daily limb usage. It is, however, a quantitative functional metric with clear clinical relevance. No established model has yet proven to be an effective predictor for clinical translation of multi-tissue interventional strategies; however, this composite injury model provides a challenging regenerative environment, rigorous and quantitative analytical methods, and clinically relevant functional deficits. This model, therefore, has unique potential to discriminate between new technologies.

There is currently no accepted standard for treatment of composite injuries, though debridement of necrotic tissue, prevention of infection, muscle flap coverage, and bone grafting are most common.<sup>6,52,53</sup> While initial assessment of healing using a muscle autograft will be important, additional strategies could utilize novel grafting materials, such as decellularized muscle tissue, which could be combined with controlled spatiotemporal growth factor delivery or progenitor cell delivery. A key component to the long-term clinical treatment of composite injuries is rehabilitation and physical loading (physical therapy); however, this is often neglected in animal models. Recently, we demonstrated that properly applied mechanical loading to a bone defect could stimulate vascular remodeling and enhance bone regeneration.<sup>54,55</sup> The muscle atrophy and functional deficits observed in this study suggest that a properly timed intervention providing physical stimulus to the injured limb may have an effect on revascularization and tissue regeneration.

This preclinical animal model uniquely combined a segmental bone defect with a volumetric muscle injury. The results showed that the increased challenge of concomitant muscle injury impaired rhBMP-2-mediated bone regeneration. Impaired limb and muscle function were also found, which are similar to clinical observations after severe composite tissue injury. Though the mechanisms involved remain unknown, there is likely a combination of mechanical and biological stimuli, both of which can serve as potential targets for intervention. This composite injury animal model provides a platform with which to analyze the mechanistic relationship of regeneration between tissues as well as test the efficacy of tissue engineering approaches to promote healing in multiple tissues. Such interventions may minimize complications and the number of surgical procedures needed for limb salvage operations, ultimately improving clinical outcomes.

### Acknowledgments

This study was supported by the U.S. Army Medical Research and Medical Command (W81XWH-10-2-0006) and the National Institute of Health (Grant # 1F32AR061236-01).

### Disclosure Statement

No competing financial interests exist.

### References

1. Edwards, C.C., Simmons, S.C., Browner, B.D., and Weigel, M.C. Severe open tibial fractures. Results treating 202 in-



- juries with external fixation. *Clin Orthop Relat Res* **230**, 98, 1988.
2. Gustilo, R.B., Merkow, R.L., and Templeman, D. The management of open fractures. *J Bone Joint Surg Am* **72**, 299, 1990.
  3. Krettek, C., Schandelmaier, P., and Tscherne, H. Nonreamed interlocking nailing of closed tibial fractures with severe soft tissue injury. *Clin Orthop Relat Res* **315**, 34, 1995.
  4. Oestern, H.J., and Tscherne, H. [Pathophysiology and classification of soft tissue damage in fractures]. *Orthopade* **12**, 2, 1983.
  5. Bosse, M.J., MacKenzie, E.J., Kellam, J.F., Burgess, A.R., Webb, L.X., Swiontkowski, M.F., *et al.* An analysis of outcomes of reconstruction or amputation after leg-threatening injuries. *N Engl J Med* **347**, 1924, 2002.
  6. Masquelet, A.C. Muscle reconstruction in reconstructive surgery: soft tissue repair and long bone reconstruction. *Langenbecks Arch Surg* **388**, 344, 2003.
  7. Utvag, S.E., Grundnes, O., Rindal, D.B., and Reikeras, O. Influence of extensive muscle injury on fracture healing in rat tibia. *J Orthop Trauma* **17**, 430, 2003.
  8. Harry, L.E., Sandison, A., Paleolog, E.M., Hansen, U., Pearse, M.F., and Nanchahal, J. Comparison of the healing of open tibial fractures covered with either muscle or fasciocutaneous tissue in a murine model. *J Orthop Res* **26**, 1238, 2008.
  9. MacKenzie, E.J., Bosse, M.J., Pollak, A.N., Webb, L.X., Swiontkowski, M.F., Kellam, J.F., *et al.* Long-term persistence of disability following severe lower-limb trauma. Results of a seven-year follow-up. *J Bone Joint Surg Am* **87**, 1801, 2005.
  10. Helgeson, M.D., Potter, B.K., Burns, T.C., Hayda, R.A., and Gajewski, D.A. Risk factors for and results of late or delayed amputation following combat-related extremity injuries. *Orthopedics* **33**, 669, 2010.
  11. Russell, W.L., Sailors, D.M., Whittle, T.B., Fisher, D.F., Jr., and Burns, R.P. Limb salvage versus traumatic amputation. A decision based on a seven-part predictive index. *Ann Surg* **213**, 473; discussion 80–81, 1991.
  12. Georgiadis, G.M., Behrens, F.F., Joyce, M.J., Earle, A.S., and Simmons, A.L. Open tibial fractures with severe soft-tissue loss. Limb salvage compared with below-the-knee amputation. *J Bone Joint Surg Am* **75**, 1431, 1993.
  13. Owens, B.D., Kragh, J.F., Jr., Macaitis, J., Svoboda, S.J., and Wenke, J.C. Characterization of extremity wounds in operation Iraqi freedom and operation enduring freedom. *J Orthop Trauma* **21**, 254, 2007.
  14. Owens, B.D., Kragh, J.F., Jr., Wenke, J.C., Macaitis, J., Wade, C.E., and Holcomb, J.B. Combat wounds in operation Iraqi freedom and operation enduring freedom. *J Trauma* **64**, 295, 2008.
  15. Liu, B. Potential for Muscle in Bone Repair. 2010.
  16. Hamrick, M.W., McNeil, P.L., and Patterson, S.L. Role of muscle-derived growth factors in bone formation. *J Musculoskelet Neuronal Interact* **10**, 64, 2010.
  17. Harry, L.E., Sandison, A., Pearse, M.F., Paleolog, E.M., and Nanchahal, J. Comparison of the vascularity of fasciocutaneous tissue and muscle for coverage of open tibial fractures. *Plast Reconstr Surg* **124**, 1211, 2009.
  18. Carano, R.A., and Filvaroff, E.H. Angiogenesis and bone repair. *Drug Discov Today* **8**, 980, 2003.
  19. Hausman, M.R., Schaffler, M.B., and Majeska, R.J. Prevention of fracture healing in rats by an inhibitor of angiogenesis. *Bone* **29**, 560, 2001.
  20. Lieberman, J.R., Daluiski, A., and Einhorn, T.A. The role of growth factors in the repair of bone. Biology and clinical applications. *J Bone Joint Surg Am* **84-A**, 1032, 2002.
  21. Chan, X.C., McDermott, J.C., and Siu, K.W. Identification of secreted proteins during skeletal muscle development. *J Proteome Res* **6**, 698, 2007.
  22. Hashimoto, N., Kiyono, T., Wada, M.R., Umeda, R., Goto, Y., Nonaka, I., *et al.* Osteogenic properties of human myogenic progenitor cells. *Mech Dev* **125**, 257, 2008.
  23. Gersbach, C.A., Guldborg, R.E., and Garcia, A.J. *In vitro* and *in vivo* osteoblastic differentiation of BMP-2- and Runx2-engineered skeletal myoblasts. *J Cell Biochem* **100**, 1324, 2007.
  24. Liu, R., Birke, O., Morse, A., Peacock, L., Mikulec, K., Little, D.G., *et al.* Myogenic progenitors contribute to open but not closed fracture repair. *BMC Musculoskelet Disord* **12**, 288, 2011.
  25. Claes, L., Maurer-Klein, N., Henke, T., Gerngro, S.S.H., Meny, M., and Augat, P. Moderate soft tissue trauma delays new bone formation only in the early phase of fracture healing. *J Orthop Res* **24**, 1178, 2006.
  26. Hamrick, M.W., Arounleut, P., Kellum, E., Cain, M., Immel, D., and Liang, L-F. Recombinant myostatin (GDF-8) propeptide enhances the repair and regeneration of both muscle and bone in a model of deep penetrant musculoskeletal injury. *J Trauma* **69**, 579, 2010.
  27. Utvag, S.E., Iversen, K.B., Grundnes, O., and Reikeras, O. Poor muscle coverage delays fracture healing in rats. *Acta Orthop Scand* **73**, 471, 2002.
  28. Histing, T., Garcia, P., Holstein, J.H., Klein, M., Matthys, R., Nuetzi, R., *et al.* Small animal bone healing models: standards, tips, and pitfalls results of a consensus meeting. *Bone* **49**, 591, 2011.
  29. Boerckel, J.D., Kolambkar, Y.M., Dupont, K.M., Uhrig, B.A., Phelps, E.A., Stevens, H.Y., *et al.* Effects of protein dose and delivery system on BMP-mediated bone regeneration. *Biomaterials* **32**, 5241, 2011.
  30. Kolambkar, Y.M., Boerckel, J.D., Dupont, K.M., Bajin, M., Huebsch, N., Mooney, D.J., *et al.* Spatiotemporal delivery of bone morphogenetic protein enhances functional repair of segmental bone defects. *Bone* **49**, 485, 2011.
  31. Kolambkar, Y.M., Dupont, K.M., Boerckel, J.D., Huebsch, N., Mooney, D.J., Huttmacher, D.W., *et al.* An alginate-based hybrid system for growth factor delivery in the functional repair of large bone defects. *Biomaterials* **32**, 65, 2011.
  32. Oest, M.E., Dupont, K.M., Kong, H.J., Mooney, D.J., and Guldborg, R.E. Quantitative assessment of scaffold and growth factor-mediated repair of critically sized bone defects. *J Orthop Res* **25**, 941, 2007.
  33. Warren, G.L., Stallone, J.L., Allen, M.R., and Bloomfield, S.A. Functional recovery of the plantarflexor muscle group after hindlimb unloading in the rat. *Eur J Appl Physiol* **93**, 130, 2004.
  34. Chu, T.M., Warden, S.J., Turner, C.H., and Stewart, R.L. Segmental bone regeneration using a load-bearing biodegradable carrier of bone morphogenetic protein-2. *Biomaterials* **28**, 459, 2007.
  35. Lieberman, J.R., Daluiski, A., Stevenson, S., Wu, L., McAllister, P., Lee, Y.P., *et al.* The effect of regional gene therapy with bone morphogenetic protein-2-producing bone-marrow cells on the repair of segmental femoral defects in rats. *J Bone Joint Surg Am* **81**, 905, 1999.
  36. Yasko, A.W., Lane, J.M., Fellingner, E.J., Rosen, V., Wozney, J.M., and Wang, E.A. The healing of segmental bone defects,

- induced by recombinant human bone morphogenetic protein (rhBMP-2). A radiographic, histological, and biomechanical study in rats. *J Bone Joint Surg Am* **74**, 659, 1992.
37. Angle, S.R., Sena, K., Sumner, D.R., Virkus, W.W., and Viridi, A.S. Healing of rat femoral segmental defect with bone morphogenetic protein-2: a dose response study. *J Musculoskelet Neuronal Interact* **12**, 28, 2012.
  38. Brown, K.V., Li, B., Guda, T., Perrien, D.S., Guelcher, S.A., and Wenke, J.C. Improving bone formation in a rat femur segmental defect by controlling bone morphogenetic protein-2 release. *Tissue Eng Part A* **17**, 1735, 2011.
  39. Schindeler, A., Liu, R., and Little, D.G. The contribution of different cell lineages to bone repair: exploring a role for muscle stem cells. *Differentiation* **77**, 12, 2009.
  40. Malizos, K.N., and Papatheodorou, L.K. The healing potential of the periosteum molecular aspects. *Injury* **36 Suppl 3**, S13, 2005.
  41. Shapiro, F. Bone development and its relation to fracture repair. The role of mesenchymal osteoblasts and surface osteoblasts. *Eur Cell Mater* **15**, 53, 2008.
  42. Dwek, J.R. The periosteum: what is it, where is it, and what mimics it in its absence? *Skeletal Radiol* **39**, 319, 2010.
  43. Einhorn, T.A. Enhancement of fracture-healing. *J Bone Joint Surg Am* **77**, 940, 1995.
  44. Gross, T.S., Poliachik, S.L., Prasad, J., and Bain, S.D. The effect of muscle dysfunction on bone mass and morphology. *J Musculoskelet Neuronal Interact* **10**, 25, 2010.
  45. Pedersen, B.K., and Febbraio, M.A. Muscles, exercise and obesity: skeletal muscle as a secretory organ. *Nat Rev Endocrinol* **8**, 457, 2012.
  46. Aliprantis, A.O., Stolina, M., Kostenuik, P.J., Poliachik, S.L., Warner, S.E., Bain, S.D., *et al.* Transient muscle paralysis degrades bone via rapid osteoclastogenesis. *FASEB J* **26**, 1110, 2012.
  47. Ausk, B.J., Huber, P., Poliachik, S.L., Bain, S.D., Srinivasan, S., and Gross, T.S. Cortical bone resorption following muscle paralysis is spatially heterogeneous. *Bone* **50**, 14, 2012.
  48. Merritt, E.K., Hammers, D.W., Tierney, M., Suggs, L.J., Walters, T.J., and Farrar, R.P. Functional assessment of skeletal muscle regeneration utilizing homologous extracellular matrix as scaffolding. *Tissue Eng Part A* **16**, 1395, 2010.
  49. Mann, C.J., Perdiguero, E., Kharraz, Y., Aguilar, S., Pessina, P., Serrano, A.L., *et al.* Aberrant repair and fibrosis development in skeletal muscle. *Skelet Muscle* **1**, 21, 2011.
  50. Evans, W.J., and Campbell, W.W. Sarcopenia and age-related changes in body composition and functional capacity. *J Nutr* **123**, 465, 1993.
  51. Perrini, S., Laviola, L., Carreira, M.C., Cignarelli, A., Natalicchio, A., and Giorgino, F. The GH/IGF1 axis and signaling pathways in the muscle and bone: mechanisms underlying age-related skeletal muscle wasting and osteoporosis. *J Endocrinol* **205**, 201, 2010.
  52. Yazar, S., Lin, C.H., and Wei, F.C. One-stage reconstruction of composite bone and soft-tissue defects in traumatic lower extremities. *Plast Reconstr Surg* **114**, 1457, 2004.
  53. Nauth, A., McKee, M.D., Einhorn, T.A., Watson, J.T., Li, R., and Schemitsch, E.H. Managing bone defects. *J Orthop Trauma* **25**, 462, 2011.
  54. Boerckel, J.D., Uhrig, B.A., Willett, N.J., Huebsch, N., and Guldberg, R.E. Mechanical regulation of vascular growth and tissue regeneration *in vivo*. *Proc Natl Acad Sci U S A* **108**, E674, 2011.
  55. Boerckel, J.D., Kolambkar, Y.M., Stevens, H.Y., Lin, A.S., Dupont, K.M., and Guldberg, R.E. Effects of *in vivo* mechanical loading on large bone defect regeneration. *J Orthop Res* **30**, 1067, 2011.

Address Correspondence to:

Nick J. Willett, PhD

Petit Institute for Bioengineering and Bioscience

Georgia Institute of Technology

315 Ferst Dr.

Atlanta, GA 30307

E-mail: nick.willett@gatech.edu

Received: May 9, 2012

Accepted: September 10, 2012

Online Publication Date: November 2, 2012